Multiple scales of shock waves in dissipative laminate materials

Pedro Franco Navarro,[1] David J. Benson,[2] and Vitali F. Nesterenko[1,3]
[1]*Department of Mechanical and Aerospace Engineering, University of California, San Diego, La Jolla, California 92093-0411, USA*
[2]*Department of Structural Engineering, University of California, San Diego, La Jolla, California 92093-0085, USA*
[3]*Materials Science and Engineering Program, University of California, San Diego, La Jolla, California 92093-0418, USA*
(Received 29 April 2016; published 15 September 2016)

The shock waves generated by a plate impact are numerically investigated in Al-W laminates with different mesostructures. The main characteristic time scales (and the corresponding spatial scales) related to the formation of the stationary shock are identified: the duration (width) of the leading front, the time (distance) from the impact required to establish a stationary profile, and the shock front width, identified as a time span (distance) from the initial state to the final quasiequilibrium state. It is demonstrated that the width of the leading front and the maximum strain rates are determined by the dispersive and the nonlinear parameters of the laminate and not by the dissipation, as is the case for uniform solids. The characteristic spatial scale of the leading front is related to the spatial scale observed on solitarylike waves, which are satisfactorily described by the Korteweg–de Vries (KdV) approximation, as well as the speed of the wave and the ratio of maximum to final strain. The dissipation affects the width of the transition distance (shock front width) where multiple loading-unloading cycles bring the laminate into the final quasiequilibrium state. This spatial scale is of the same order of magnitude as the distance to form stationary shock wave. The period of fast decaying oscillations is well described by the KdV approach and scales linearly with the cell size. The rate of the decay of the oscillations in the numerical calculations does not scale with the square of the cell size as expected from the dissipative KdV approach that assumes a constant viscosity. This is due to the different mechanisms of dissipation in high-amplitude compression pulses.

DOI: 10.1103/PhysRevE.94.033002

I. INTRODUCTION

The response of nonlinear materials with periodic microstructure depends on the parameters of the incoming disturbance. For example, short-duration pulses result in solitary waves, longer pulses can produce a train of solitary waves or shocklike stress pulses, and periodic excitations result in strongly nonlinear periodic waves in granular chains [1,2]. The balance of weak nonlinearity and dispersion caused by a periodic microstructure results in small-amplitude solitarylike waves (stegotons) in nondissipative laminates [3]. In Ref. [4] incoming, short, high-amplitude pulses (with respect to the characteristic inner time scale determined by the cell size and the sound speed of components) generated weakly decaying compression solitarylike waves in the dissipative nonlinear Al-W laminate.

In this paper we analyze the transient and quasisteady responses of dissipative Al-W laminates to long-duration, high-amplitude incoming pulses allowing the establishment of steady shock wave profiles and quasiequilibrium states behind the shock front. The response to high-amplitude shock loading of homogeneous materials is usually analyzed assuming that at high-amplitude loading, a steady state behind the shock exists. This approach ignores the transient stage necessary to establish a stationary shock front and does not account for the possible maximum in stresses reached during the intermediate stages preceding a steady state behind the shock. The establishment of a steady shock wave is assumed to happen when it has propagated for at least a few shock front widths [2,5]. The assumption of a steady shock wave allows the use of conservation laws across the shock front, which results in the Rankine-Hugoniot equations connecting the states behind and in front of the stationary shock wave [5–7]. In laminate materials, the establishment of a steady state behind the wave and steady propagation regime might not occur, as can be seen in the case of short-duration incoming pulses. The examples include powerful laser loading, impact by small thickness plates, or contact explosion [8,9]. Some approaches to create Hugoniot curves for mixtures (with different degrees of success) are reviewed in [10], though they usually do not address the spatial scales of the shocked materials when they are applicable. The assumption that the shock wave has reached a steady state might be incorrect, at least in cases when characteristic duration of the shock wave is about the characteristic time of pulse propagation through the cell [4,11]. The shock wave propagation in finite nonlinear laminates can result in peculiar and counterintuitive effects such as the increase of amplitude of the wave with the decrease of layer thickness; this contradicts the behavior based on the difference of acoustic impedances of linear elastic materials [2,12,13].

The dissipation processes during shock loading and nonlinearity of material behavior determine the width of the shock wave in homogeneous materials [14–17]. In homogeneous materials for strong shock waves, the fourth power law was established to relate the maximum strain rate and stress behind the shock in the form $\dot{\epsilon} = \alpha\sigma^4$, where $\dot{\epsilon}$ represents the strain rate at the leading front and σ the maximum stress on the leading front. This result was introduced by Grady and a thorough explanation can be found in [18,19]. This fourth power law has been widely adopted in the shock physics community. Nevertheless, experimental results presented in the paper by Zhuang *et al.* [20] demonstrated that this law does not apply to laminate materials. Instead, a second power law, i.e., $\dot{\epsilon} = \alpha\sigma^2$, was proposed to connect the maximum stress and strain rate.

It was shown in [4,11] that the nature of high-amplitude stress waves in dissipative Al-W laminate was determined by the ratio of the duration of incoming pulses to the characteristic time of pulse propagation through the cell ($t_r = \frac{2d_{\text{imp}}}{C_{\text{imp}}} / \frac{d_{\text{lam}}}{C_{\text{lam}}}$),

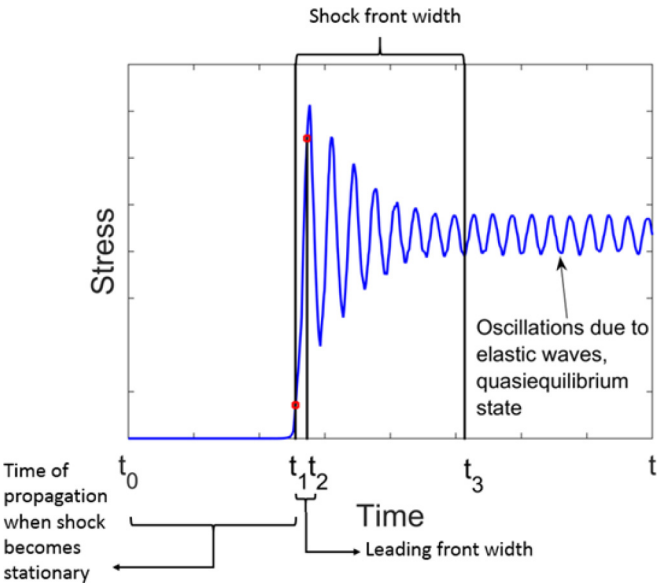

FIG. 1. Three characteristic time scales related to the established stationary shock profile detected at some point inside the laminate far enough from the impacted end. The three time scales identified in the graph are described as follows: time of propagation t_1-t_0 when the shock excited by an external disturbance at time t_0 becomes stationary (it has achieved a steady amplitude and width of the leading front as well as an oscillating profile of the shock and final state), shock front width t_3-t_1 determined by the time difference corresponding to 0.1 of the maximum stress amplitude and time when plastic deformation is replaced by slowly decaying elastic reverberations (quasiequilibrium state), and leading front width t_2-t_1 determined by the time difference between a point with a maximum stress amplitude of 0.1 and a point with a maximum stress amplitude of 0.9. The latter time difference should be used to determine the maximum strain rate in the stationary shock.

where C_{lam} is the equivalent sound speed in the laminate; in this paper C_{lam} has a value of 3381 m/s, being the limit of the long-wave approximation expressed by Eq. (4). At small time ratios ($t_r < 2.5$), numerical calculations demonstrated that the incoming pulse was localized after a propagation distance of about four to five cells. Its properties (speed and shape) were similar to a weakly nonlinear Korteweg–de Vries (KdV) solitary wave. Longer incoming pulses ($t_r > 5$) were transformed into a train of separated solitarylike waves or into a triangular oscillatory shock profile depending on the level of dissipation. Preliminary results related to the scaling of the shock wave loading can be found in [11].

In this paper we investigate numerically the multiple scales of high-amplitude shock waves generated by the plate impact in Al-W laminates with different mesostructures. We identify three different characteristic time scales presented in Fig. 1 related to the formation of the stationary shock: the time from the impacted end required to establish a stationary shock profile, the width of the leading front determining the maximum strain rate of loading, and the width of the shock wave identified as the time span from the initial state to the final equilibrium (quasiequilibrium) state (slowly attenuating elastic vibrations can still be present as well as differences in the temperatures of Al and W).

The establishment of this stationary wave profile takes some propagation distance depending on the cell size and properties of components. In the first few cells, the leading pulse is still a shock waves in individual components [4,11–13] and not part of a stationary shock wave in the laminate. The transition from the initial to the final equilibrium state in the Al laminate with gaps (modeling porous materials) due to multiple reverberations of shock waves was numerically demonstrated in [14].

The schematic of the shock wave structure presented in Fig. 1, strictly speaking, does not represent a final state due to presence of oscillating elastic waves that have not decayed; this state also has different temperatures in the components. We can characterize this final state as a frozen state with a time scale to reach equilibrium much longer than the characteristic times of wave propagation in practical devices. Nevertheless, the decay of the elastic reverberations and the equilibration of the temperature between the components will probably have only a slight effect on the final stress and particle velocity. The characteristic times related to the attenuation of the elastic oscillations and the even longer time required for thermal equilibrium are not shown in Fig. 1. These characteristic scales might be relevant for the nanolaminates.

The state in the leading front is a transient state and should not be used as the final state of the laminate Hugoniot. It should be mentioned that the Hugoniot curve has no information on the type of dissipative processes leading to the establishment of the final equilibrium state. The parameters that the leading front depends on are the specific dissipative properties of individual components of the laminate and, depending on them, it can be different with the same final equilibrium state.

It was demonstrated that in the investigated Al-W laminate that the width of the leading front (and subsequently time interval t_2-t_1) is mostly determined by the laminate's mesostructure, nonlinear parameters of components, and amplitude of the shock. This time scale can be related to the characteristic scale of the solitarylike wave observed in [4] that is satisfactorily described by the Korteweg–de Vries approximation [4,11]. The critical level of dissipation corresponding to the transition of an oscillatory to a monotonic shock (as in Fig. 1) is determined by the amplitude of the wave and the dispersive properties of laminates similar to the stress wave profiles in discrete dissipative granular chains [1,2]. The dissipation affects the width of the shock front, during which multiple loading cycles bring the laminate into a final quasiequilibrium state. This time scale is of the same order as the propagation time to form a stationary shock wave in the investigated Al-W laminate.

It is appropriate to mention that the shock wave solution of the KdV equation with viscous dissipation has two space scales. For weak dissipation, the shock front width is determined by the nonlinear effects and depends on the shock amplitude and the dispersion coefficient, unlike the characteristic size of the shock front width that is determined by viscous dissipation and dispersion. The characteristic size of the oscillations behind the shock front is of the same order as the width of the leading front width.

II. SIMULATIONS

One-dimensional numerical calculations were performed using LS-DYNA, a general-purpose finite-element program

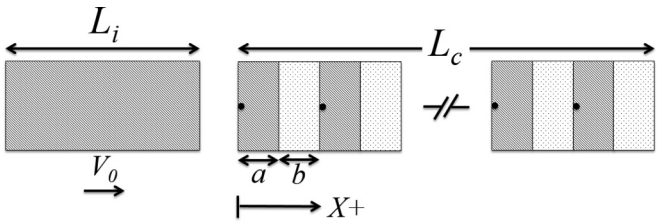

FIG. 2. Geometry of laminate Al-W material. Black dots indicate points in Al layers adjacent to the interfaces where the stress is calculated.

[21] used in [4]. The material response was modeled with the Steinberg-Guinan plasticity model coupled with Grüneisen's equation of state [22,23]. The experimental results of the homogeneous materials (Al and W) were compared to the results of the numerical calculations to verify the agreement of temperature and stresses at the final state of the material behind the shocks with published Hugoniot data.

The components in the laminates (see Fig. 2) had equal thicknesses ($a = b$) with values of a and b equal to 2, 1, and 0.5 mm. All the layers were modeled as perfectly bonded, which is an appropriate assumption for compression wave loading. In this paper striker plates with relatively large thicknesses ($L_i =$ 80 and 800 mm) were used to create long-duration incoming pulses with a time ratio t_r ranging from 25 to about 1000.

The mesh size in all cases was equal 1×10^{-5}m $= 0.01$mm and the selected artificial viscosity resulted in a shock width in Al and W at least ten times smaller than the smallest layer size (0.5 mm). This ensures that a steady state is reached behind the shock waves when they propagate inside each layer during the initial stage of the pulse formation following the impact. Of course, it is desirable that the numerical shock width is similar to the one found in experiments [24,25], but the width of the shock front is not important for the parameters of the final state as long as the shock width is sufficiently smaller than the layer thickness. This ensures that the material reaches Hugoniot states at each shock loading. The Hugoniot states are characteristic of stationary shocks and are independent of the specific mechanisms of dissipation only defining the width of the transient zone. In our calculations the plastic shock width Δx and the rise time Δt are, for aluminum, $\Delta t = 3.72 \times 10^{-9}$s and $\Delta x = 3.38 \times 10^{-5}$m (at a shock stress of 70 GPa) and for Tungsten, at the same shock stress, the shock rise time is $\Delta t = 9.69 \times 10^{-9}$s and $\Delta x = 4.79 \times 10^{-5}$m. Both of the shock widths are about 10 times smaller than the smallest cell size (0.5 mm) used in the laminate and are much smaller than the characteristic scale of oscillations observed in the shock wave.

III. RESULTS OF NUMERICAL CALCULATIONS

The results of one-dimensional numerical calculations related to the formation and propagation of stress pulses generated by a long duration of incoming disturbances, with time ratios t_r between 25 and 1015, are investigated in this paper. At these higher time ratios, unlike in previous study [4], a stationary shock wave with an oscillating tail, where the frequency of the oscillations changes with the size of the cell, can be observed. We present results related to the formation and propagation of shock waves in 2+2 (2 mm Al plus 2 mm W layers), 1+1 (1 mm Al plus 1 mm W layers), and 0.5+0.5 (0.5 mm Al plus 0.5 mm W layers) laminates impacted by 80- and 800-mm Al flyer plates. The numerical data presented here correspond to a point in the Al layers right at the interface with the W layers and (Fig. 2) all the distances are measured from the impacted end.

A. A 2+2 laminate impacted by an 80-mm Al flyer plate ($t_r = 25$)

The stress evolution in a shock wave propagating in a 2+2 laminate impacted by an 80-mm Al plate is presented in Figs. 3(a) and 3(b). From these figures we can observe that at a depth of 12 mm, the duration of the leading front was already close to its stationary value (evident at a larger depths). We will later show how this corresponds to half of the duration of the stationary solitarylike wave presented in [4] and thus can be approximated by analytical equations presented in [4,11];

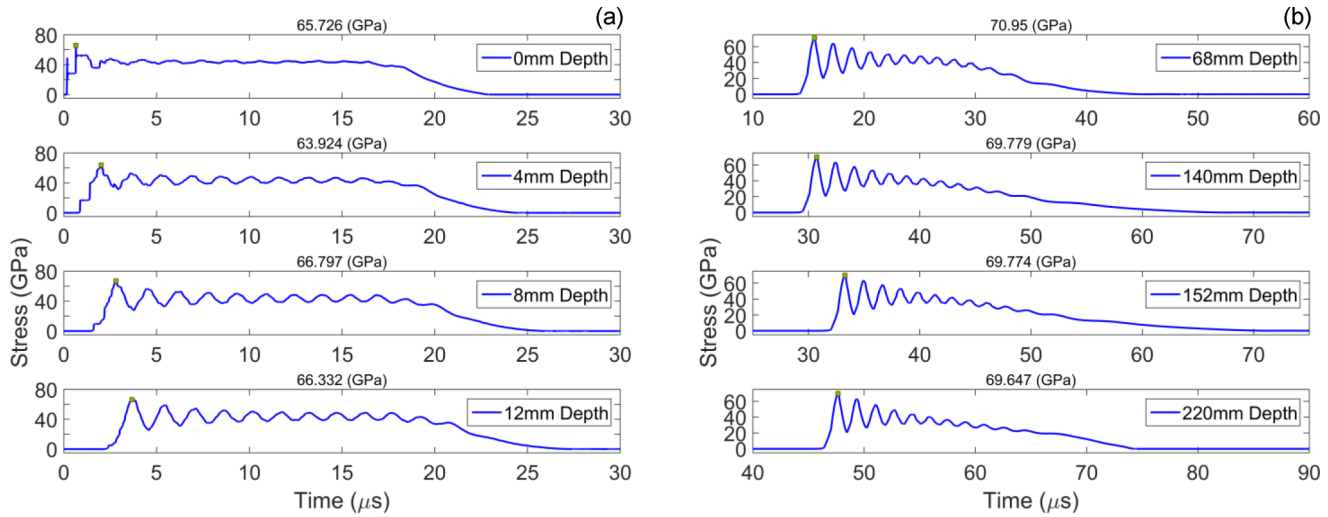

FIG. 3. Stress pulse evolution in a 2+2 laminate impacted by a 80-mm Al flyer plate at 2800 m/s at different distances from the impacted end: (a) 0, 4, 8, and 12 mm and (b) 68, 140, 152, and 220 mm.

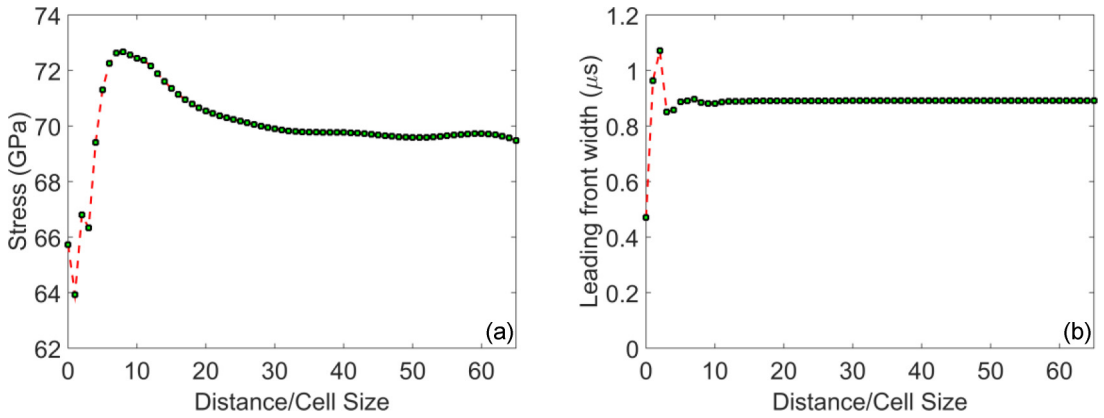

FIG. 4. A 2+2 laminate impacted by a 80-mm Al flyer plate at 2800 m/s. (a) Maximum stress on the leading front of the shock versus distance from the impacted end. (b) Leading front width versus distance from the impacted end.

from these equations, the width of the leading part of the shock can be determined.

It is clear that the relatively fast decaying stress oscillations, due to plastic deformation, exist immediately behind the leading front (four first pulses). The amplitude of these oscillations initially increases with the propagation distance until they become quasistationary at some depth, as shown by the leading oscillations in the stress profiles in Fig. 3(b). This is typical for the dispersive behavior of materials with periodic mesostructures and weak dissipation, e.g., granular chains [26].

The mostly elastic oscillations behind the shock front attenuate very slowly. For this impact condition, they did not oscillate around an established mean value before the arrival of the release wave from the free surface of the impactor. It is interesting that the amplitude of elastic oscillations decreased with the arrival of the rarefaction wave due to their compressive nature. Thus the quasiequilibrium state, under this impact condition, was not reached and the use of the Hugoniot curve is not appropriate to describe the final states behind shock in the laminate.

It is interesting that the amplitude of the leading pulse has reached practically steady values (which we define as a deviation from the mean value that is below 0.5%) at a distance of about 120 mm [Fig. 4(a)]. The stationary leading front width and the amplitude of the leading pulse were reached despite the fact that the quasiequilibrium state behind shock (Fig. 1) was not established due to the arrival of the rarefaction wave. The leading front [0.1–0.9 wide (Fig. 1)] of the oscillatory shock wave approaches a stationary value at a distance of 25 mm [Fig. 4(b)]. It seems that reaching the steady values of the leading amplitude is a slower process than establishing a leading front width. This is probably due to the different mechanisms determining their establishment, where the latter is mainly caused by the balance of the nonlinear and the dispersive terms and the former is due to a slower dissipation processes. We will illustrate that by using the KdV weakly dissipative approach it is possible to approximate the leading front width.

The speed of the shock when the leading pulse reached its steady amplitude is equal to 4729 m/s. The nature of the shock wave and that of the solitary wave are qualitatively different. It is reflected in their different speeds of propagation; a solitarylike wave at the same stress level (∼70 GPa) in the same Al-W laminate has a speed of 4474.5 m/s [4].

Figure 5 presents a comparison of the solitary wave profile in a 2+2 laminate with the real dissipative properties [4] hit by the 8-mm Al plate with a velocity of 2800 m/s and the profile of the shock wave with a similar stress amplitude generated in the same laminate by the impact of the Al plate with a thickness of 80 mm. The comparison of the two stress profiles clearly shows that the shape and width of the leading stationary front of the shock are closely approximated by the solitarylike wave. Thus the strain rates in the leading part of the shock wave can be estimated based on the properties of the solitarylike waves presented in [4,11].

B. A 2+2 laminate impacted by an 800-mm Al flyer plate ($t_r = 254$)

In the previous section we observed that the impact on a 2+2 laminate by an 80-mm Al plate did not form a stationary shock wave due to the relatively short duration of the incoming pulse

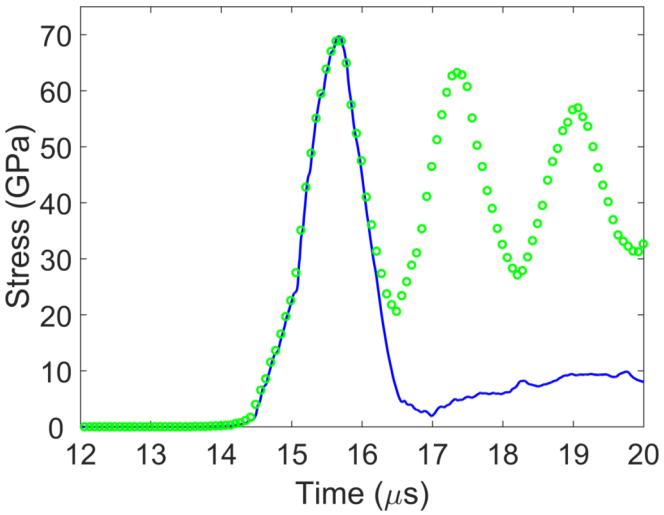

FIG. 5. Comparison of a solitarylike wave (solid line) and leading part of a shock wave (open circles) in the same 2+2 Al-W laminate. The solitarylike wave was created by the impact of an 8-mm Al flyer plate [4] while the shock wave was created by the impact of an 80-mm Al flyer plate.

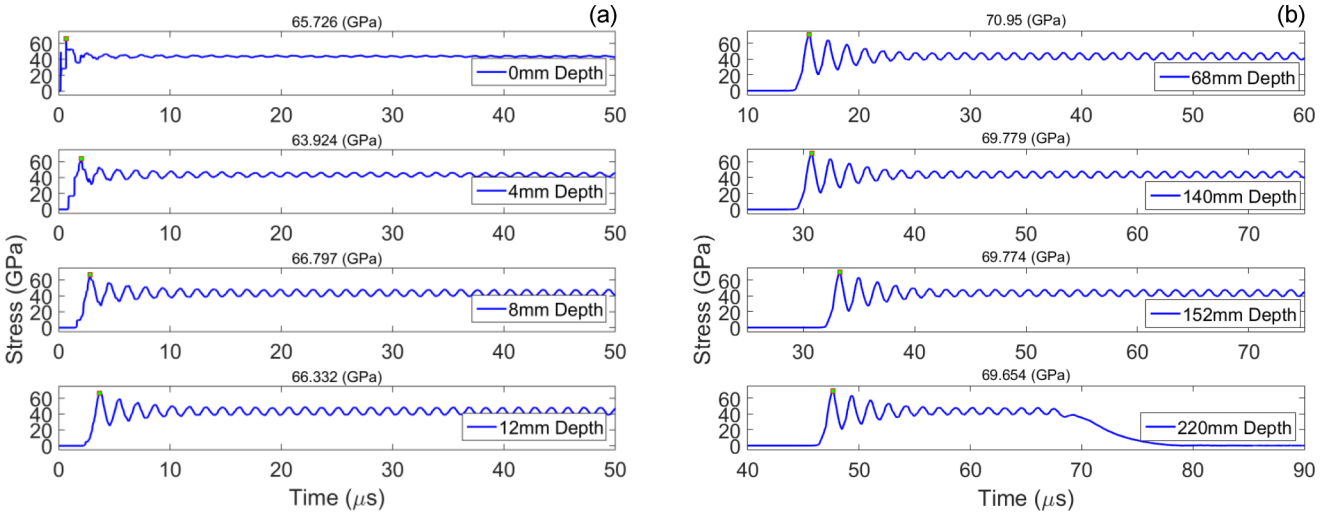

FIG. 6. Stress pulse evolution in a 2+2 laminate impacted by an 800-mm Al flyer plate at 2800 m/s at different distances from the impacted end: (a) 0, 4, 8, and 12 mm and (b) 68, 140, 152, and 220 mm.

in comparison with the characteristic time scale of the laminate. To increase the duration of the incoming pulse and explore its influence on the wave structure, an impact by an 800-mm Al plate with a velocity of 2800 m/s on a laminate with an identical mesostructure (2+2, as in the previous case) was investigated. These impact conditions correspond to a time ratio of $t_r = 254$. The impact conditions were selected to remove the influence of the rarefaction wave in an attempt to reach a quasiequilibrium state behind the stationary shock front.

The evolution of the stress pulses is presented in Fig. 6. As in the case of the 2+2 laminate impacted by the 80-mm Al flyer plate, at a depth of 12 mm, the leading front with similar amplitude was already close to its stationary value. Relatively fast decaying oscillations of the stress due to the plastic deformation exist right behind the leading front (the four first pulses), reflecting the dispersive behavior of the materials with periodic mesostructures and weak dissipation, e.g., granular chains [1,26].

Despite a different duration of the incoming pulse between this case and the previous one (impact by an 80-mm Al plate), the establishment of the leading front width of the shock wave and a steady amplitude of the leading peak happened at similar distances (compare Figs. 4 and 7). This demonstrates that at the investigated ranges of time ratios $t_r = 25-254$, a quasisteady shock front with an oscillatory tail can be expected, although reaching this quasisteady state takes a distance of about 120 mm (30 cells) or 25 mm (about 6 cells) for the leading amplitude and leading front width correspondingly. It should be emphasized that at much shorter time ratios ($t_r = 0.25$) qualitatively different disturbances (solitarylike pulses) were observed [4].

In contrast to the previous case with an impact by an 80-mm Al plate, the quasiequilibrium state was indeed reached behind the leading part of the shock front with mostly elastic, very slowly attenuating oscillations about an established mean value. The elastic nature of these oscillations is demonstrated in Fig. 8, which shows the evolution of the shock front width with the traveling distance [Fig. 8(a)] and the stress history with its corresponding effective plastic strain at a depth of 100 mm from the impacted end [Fig. 8(b)]. The shock front width is determined by the distance from the leading edge of shock wave to the point where plastic strain is saturated.

This quasiequilibrium state behind the shock (there are still elastic oscillations and different temperatures in the

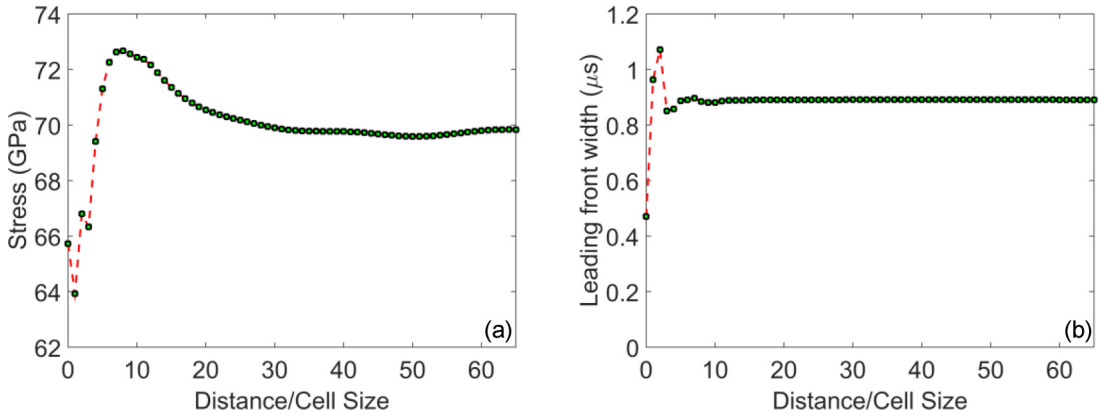

FIG. 7. A 2+2 laminate impacted by an 800-mm Al flyer plate at 2800 m/s. (a) Maximum stress in the leading peak vs propagation distance. (b) Leading front width versus propagation distance.

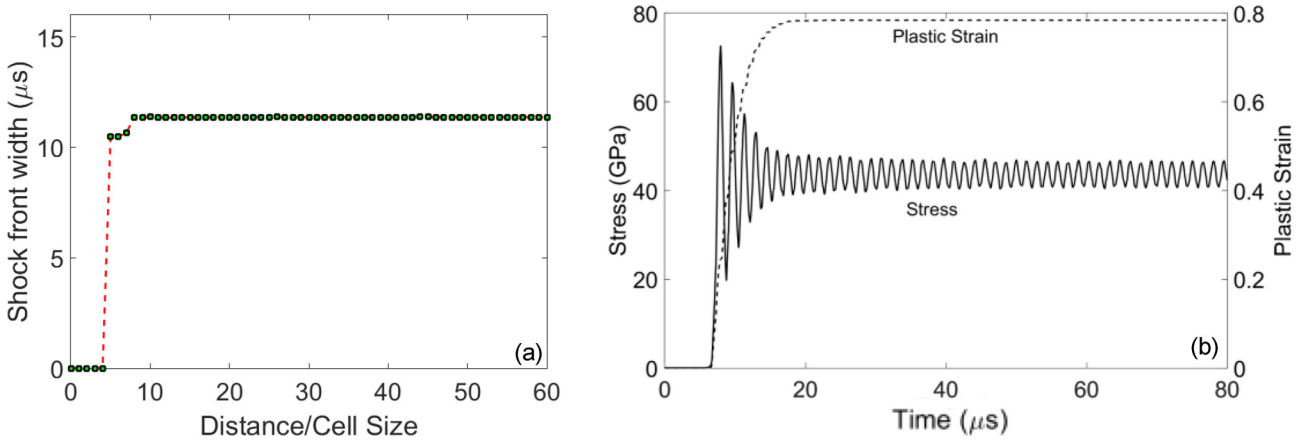

FIG. 8. A 2+2 Al laminate impacted by an 800-mm Al flyer plate at 2800 m/s. (a) Shock front width vs traveled distance. (b) Superposition of stress profile and effective plastic strain; the inflection point on the plastic strain curve (right Y axis) indicates the point where oscillations become purely elastic.

components) and the established mean value of the stress can be approximated using the equation for the normal stress ($\sigma = \rho_0 Du$) based on the stationary conditions of the shock front and the assumption of a quasiequilibrium state behind the shock front. Indeed, using the initial density of the laminate ($\rho_0 = 11\,043\,\mathrm{kg/m^3}$), the particle velocity ($u = 827\,\mathrm{m/s}$), and the shock speed ($D = 4279\,\mathrm{m/s}$), a normal stress behind the shock is calculated to be 43.2 GPa, compared to 43.42 GPa from the numerical simulations.

The quasiequilibrium state was reached by a sequence of attenuating oscillations. These oscillations have a characteristic decay time that is determined by the dissipation mechanism. In our case, this is mostly plastic deformation. The structure of the stress pulse is qualitatively similar to the one expected for dispersive and weakly dissipative media described by the KdV equation with viscous dissipation. The characteristic scale in this approach is determined by the viscosity and dispersive coefficients [27,28].

The oscillating behavior continues into the quasiequilibrium state characterized only by elastic deformation. When the 2+2 laminate has reached a quasiequilibrium state, the compressed cell thickness is 3.3 mm: 1.5 mm Al plus 1.8 mm W. Sound speeds in the compressed components are 7942 m/s for Al and 4700 m/s for W [5] compared to their original 5328 and 4030 m/s, respectively. By using the corresponding sound speed of each layer under compression, we calculate the new long-wave sound speed in the compressed laminate to be 4910 m/s. The characteristic time of the sound propagation through the compressed cell is 6.7×10^{-7}s, about two times smaller than period of the elastic oscillations in the quasiequilibrium state. These oscillations are probably the remnants of the oscillations inside the shock front where the plastic deformation provides the mechanism of their attenuation. The period of the elastic oscillations is scaled with the thickness of the laminate cell; for example, in the 2+2 laminate, the period is 15×10^{-7}s and in the 1+1 laminate

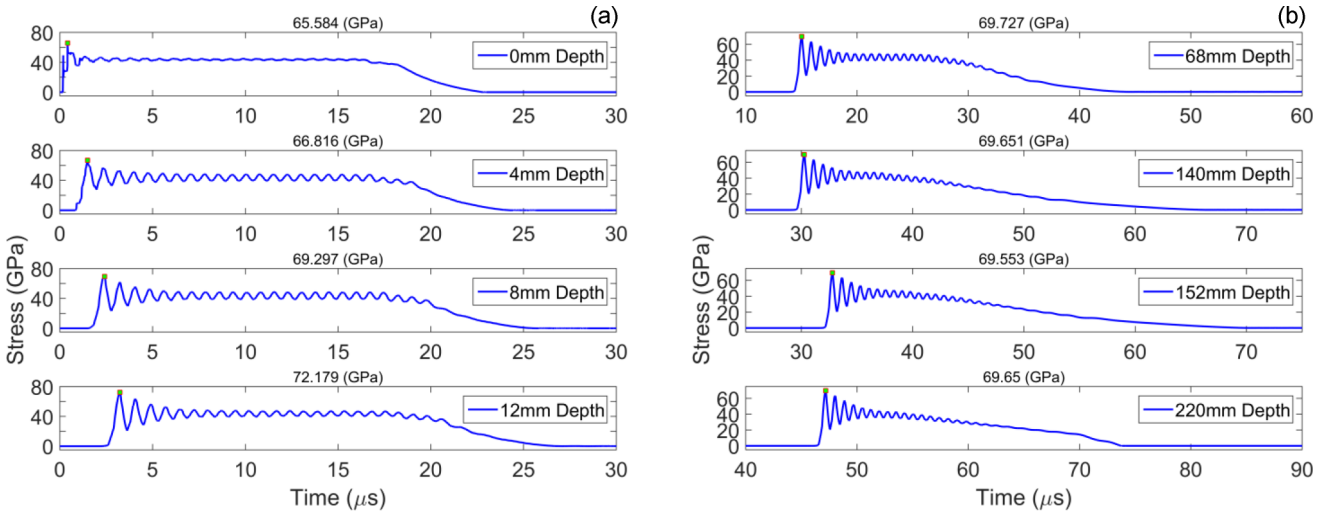

FIG. 9. Stress pulse evolution in a 1+1 laminate impacted by an 80-mm Al flyer plate at 2800 m/s at different distances from the impacted end: (a) 0, 4, 8, and 12 mm and (b) 68, 140, 152, and 220 mm. Compare these profiles with the waves structure in the 2+2 laminate excited by the same Al plate.

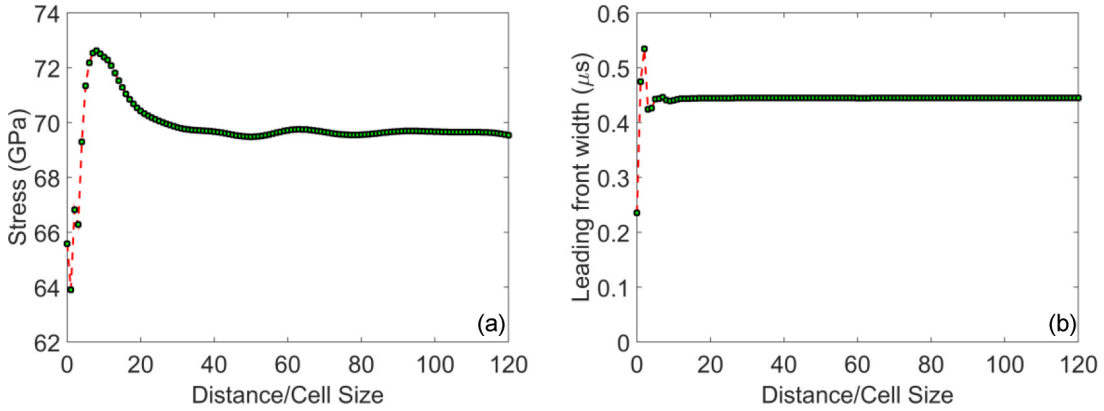

FIG. 10. Establishment of the stationary amplitude in the leading front in the 1+1 laminate impacted by an 80-mm Al flyer plate at 2800 m/s: (a) maximum stress in the leading peak vs propagation distance and (b) leading front width versus propagation distance.

presented later (Fig. 9), the period is 7.4×10^{-7}, about two times smaller at similar amplitudes of the leading wave and similar mean value of the stress in the quasiequilibrium state behind shock.

C. A 1+1 laminate impacted by an 80-mm Al flyer plate ($t_r = 51$)

In Sec. III A it was demonstrated that the impact by an 80-mm Al plate on the 2+2 laminate did not generate a stationary shocklike stress pulse. The dispersive properties of the laminates depend on the cell size and it is expected that this parameter can influence the rate of the establishment of the stationary shock wave. To explore the effects that cell refinement might have on the length scales required for the establishment of a stationary front, a refined 1+1 laminate, impacted by an 80-mm Al flyer plate (as in Sec. III A) was investigated.

Figures 9(a) and 9(b) show the results of the stress wave evolution inside this laminate. A few features should be emphasized. As in the previous cases, the stress waves have oscillatory profiles. However, in this case, the quasistationary stress wave (with elastic oscillations in the quasiequilibrium state) was formed, unlike the transient waves in the 2+2 laminate excited by the impact of the same 80-mm Al plate.

A difference in the frequency of oscillations behind the leading front of the wave can be observed by comparing the wave profiles presented in Figs. 3(a) and 3(b) and Figs. 9(a) and 9(b). It indicates that cell size is directly related to the period of these oscillations.

Another important feature of the stress waves in this refined 1+1 laminate is the faster establishment of the stationary leading front in comparison with the coarser 2+2 laminate [compare Figs. 3(a) and 9(a)]. In the former case, the stationary leading front and quasiequilibrium state behind, with oscillations fluctuating around a mean value of 43.6 GPa, were formed at relatively short distances from the impacted end (12 mm). At the same distance from the impacted end, in the 2+2 laminate, the stress wave did not have a stationary leading front and the establishment of the quasiequilibrium state behind it was already influenced by the rarefaction wave.

The following details of the establishment of the stationary state of the leading front should be mentioned. By inspection of Figs. 9(a) and 9(b), one can qualitatively observe that a maximum steady stress level of approximately 69 GPa has been reached. Figure 10(a) presents a detailed picture of this process, demonstrating that this steady stress level is reached relatively close to the impacted end (at about 60 mm), compared to the corresponding distance of 120 mm in the case of the 2+2 laminate impacted by the 80- or 800-mm Al plates, where the same level of maximum stress in the leading front was observed.

The leading front width is scaled with the cell size and it is equal to 0.445 μs (the 1+1 laminate [Fig. 10(b)]) compared to 0.89 μs in the 2+2 laminate. It is important to analyze whether or not this 1+1 laminate has reached a quasiequilibrium state behind the shock front for these impact conditions (Fig. 11). The formation of the quasiequilibrium state behind the shock front was not observed in the case of the 2+2 laminate, impacted by the 80-mm Al flyer plate (Fig. 3). Refinement of the cell size helped us reach a steady shock wave with a steady amplitude in the leading front; widths of the leading and shock wave fronts were established before the arrival of the rarefaction wave (Figs. 10 and 11).

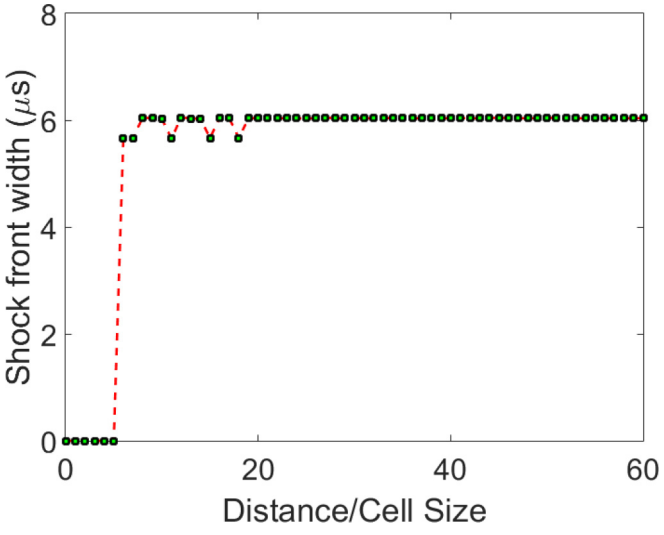

FIG. 11. Establishment of the stationary shock front width with traveled distance in a 1+1 Al laminate impacted by an 80-mm Al flyer plate at 2800 m/s.

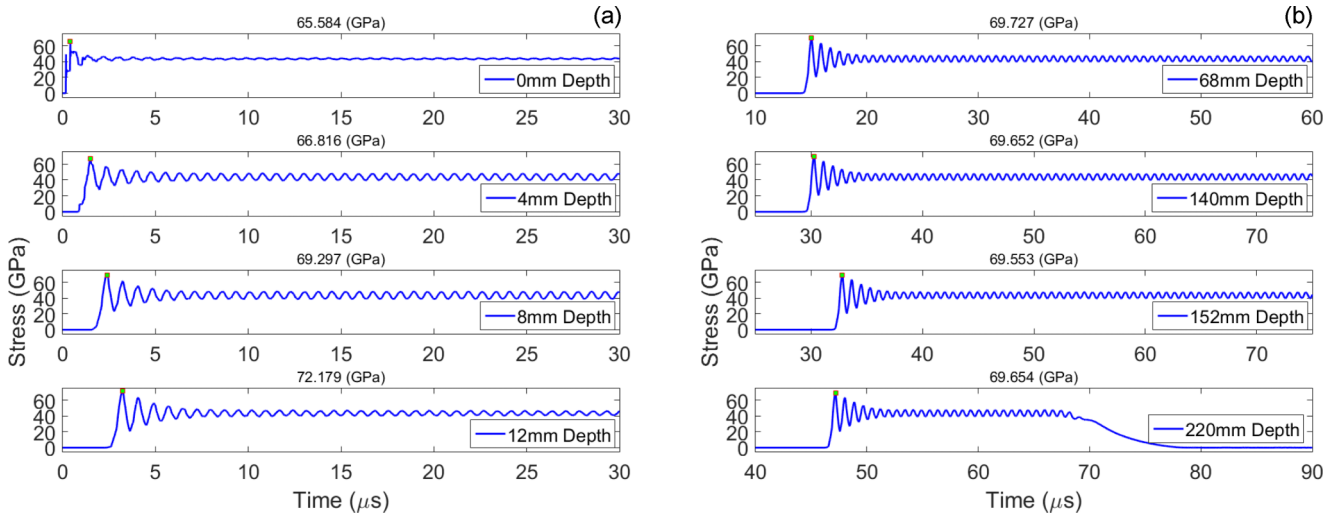

FIG. 12. Stress pulse evolution in a 1+1 laminate impacted by an 800-mm Al flyer plate with a velocity of 2800 m/s at different distances from the impacted end: (a) 0, 4, 8, and 12 mm and (b) 68, 140, 152, and 220 mm.

D. A 1+1 laminate impacted by an 800-mm Al flyer plate ($t_r = 508$)

We now explore if a longer duration incoming pulse than in the previous section results in the same parameters (amplitude of the leading shock front, leading front width, and shock front width) of the shock wave in the 1+1 laminate. To generate a longer incoming pulse in the 1+1 laminate, the numerical calculations were conducted with an 800-mm Al flyer plate having a velocity of 2800 m/s. Figures 12(a) and 12(b) present the results of these numerical simulations.

Figures 12(a) and 12(b) show that the final quasiequilibrium state (where elastic oscillations are present) was reached before the arrival of the release wave. It is interesting that these oscillations very quickly decay after the arrival of the release wave. The oscillations are around the same mean value of the normal stress (43.6 GPa) as in the previous cases (the 1+1 laminate impacted by the Al plate with an 80-mm thick plate [Fig. 9(a)] and 2+2 laminate impacted by an 800-mm Al plate [Fig. 6(b)]), where the quasiequilibrium state was reached behind the shock wave. The comparison of the final states behind the shock waves propagating in different laminates clearly demonstrates that the final quasiequilibrium state is not sensitive to the laminate's mesostructure.

It is interesting to find the distance where a steady shock front was established in this fine laminate. Figures 13(a) and 13(b) show the dependence on propagation distance of the stress at the leading peak and the leading front width of the shock. It is clear that they reached steady state values at different distances, which are the same as in the case of the 1+1 laminate impacted by the 80-mm Al plate [Figs. 10(a) and 10(b)].

A comparison of Figs. 10 and 13 demonstrates that a longer impactor (bigger time ratio t_r) did not affect the distance from the impacted end necessary for the establishment of the leading front width and the maximum stress level at the leading peak. This observation suggests that there is a critical time ratio at which a stress wave in a laminate will be able to reach a steady-state regime. The normalized propagation distance to establish the steady peak stress was similar in the 2+2 and 1+1 laminates [about 30 cells in both cases; compare Figs. 7(a) and 13(a)]. The leading front width also scaled with the size of the cell, resulting in times equal to 0.45 μs in the 1+1 laminate vs 0.9 μs in the 2+2 laminate.

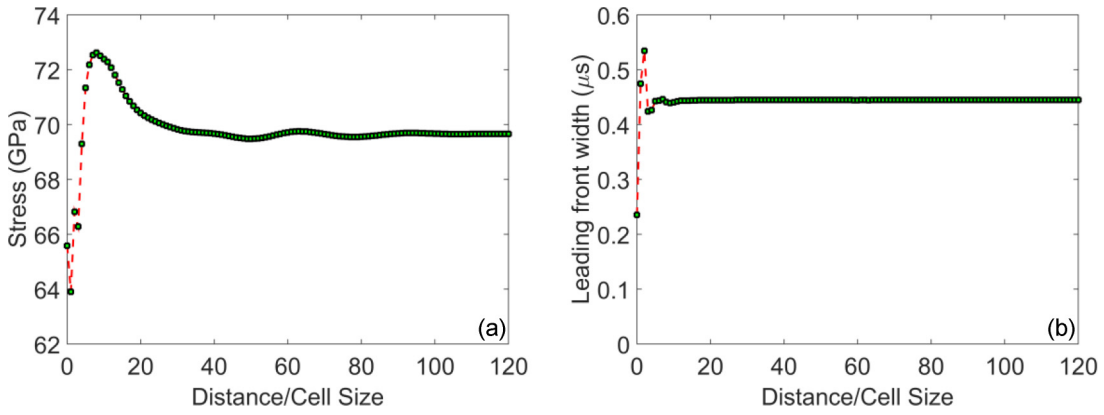

FIG. 13. (a) Maximum stress in the leading peak and (b) leading front width versus propagation distance in a 1+1 laminate impacted by an 800-mm Al flyer plate at 2800 m/s.

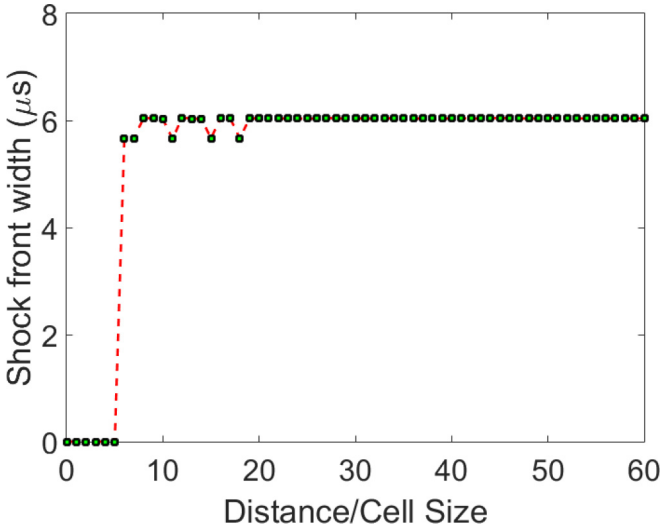

FIG. 14. Shock front width vs traveled distance in the 1+1 Al laminate impacted by an 800-mm Al flyer plate at 2800 m/s.

Figure 14 illustrates the establishment of a steady shock front width in the 1+1 Al laminate impacted by an 800-mm Al flyer plate. The shock front width also scaled with the laminate cell size, decreasing from 11.4 μs in the 2+2 laminate to 6 μs in the 1+1 laminate [compare Fig. 14 to Fig. 8(a)]. The oscillations in the quasiequilibrium state behind the steady shock front in the 1+1 laminate have a period half as large as the ones found in the 2+2 laminate (compare Figs. 6 and 12).

E. A 0.5+0.5 laminate impacted by an 80-mm Al flyer plate ($t_r = 102$)

It was shown that the impact by the 80-mm Al flyer plate on a 1+1 laminate [Figs. 9(a) and 9(b)] resulted in a steady shock at a distance of about 30 cell sizes (Figs. 10 and 11), while at the same impact conditions, a steady shock wave was not formed in a 2+2 laminate at the same normalized distance from the impacted end [Figs. 3(a) and 3(b)]. We now explore if a steady shock is formed in a finer (0.5+0.5) laminate and how the main space-time scales change with the cell size. Figures 15(a) and 15(b) present the stress evolution in this 0.5+0.5 laminate impacted by an 80-mm Al flyer plate.

From the evolution of the stress wave profile, it is clear that a steady shockwave is established. It is important to compare the distance to establish the steady shock with results for the 1+1 laminates impacted by the same flyer plate. Figure 16(a) shows that the stress at the leading front reached a stationary value at around 30 cells, which is consistent with the previously analyzed 1+1 laminate [Fig. 10(a)]. The leading front width has also scaled with the refinement of the cell size as can be observed in Fig. 16(b).

The establishment of the shock front width is shown in Fig. 17. Contrary to other laminates, we observe bigger fluctuations before reaching a steady value close to 4 μs.

It is interesting that the normalized distance for the establishment of steady shock front width in the 0.5+0.5 laminate is similar to the case of the 1+1 laminate, but variations of this parameter inside the transient range are much larger in the former laminate (compare Figs. 11 and 17). Thus we can conclude that impact by the 80-mm flyer plate resulted in the establishment of a steady shock wave at the same amplitudes and similar normalized space scales in the 1+1 and 0.5+0.5 laminates. Similar impact conditions did not result in a steady shock wave in the 2+2 laminate.

F. A 0.5+0.5 laminate impacted by an 800-mm Al flyer plate ($t_r = 1016$)

It is natural to expect that an increase in the duration of the incoming pulse in the 0.5+0.5 laminate, generated by impact of the 800-mm flyer plate, will also result in the establishment of a steady shock wave. Nevertheless, we want to check if the amplitude of this wave will be similar to the case of the impact by the 80-mm flyer plate at the same velocity and if characteristic length scales for the shock wave will be the same. In other words, we would like to explore if a steady shock wave in the 0.5+0.5 laminate does not depend on the relatively long

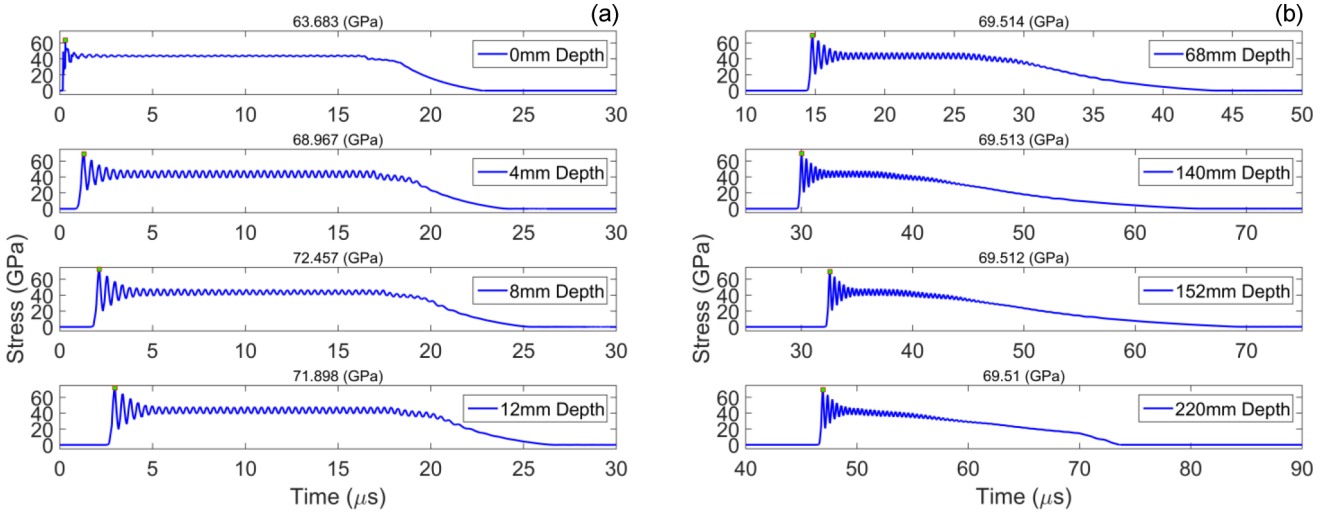

FIG. 15. Stress pulse evolution in a 0.5+0.5 laminate impacted by an 80-mm Al flyer plate at 2800 m/s at different distances from the impacted end: (a) 0, 4, 8, and 12 mm and (b) 68, 140, 152, and 220 mm.

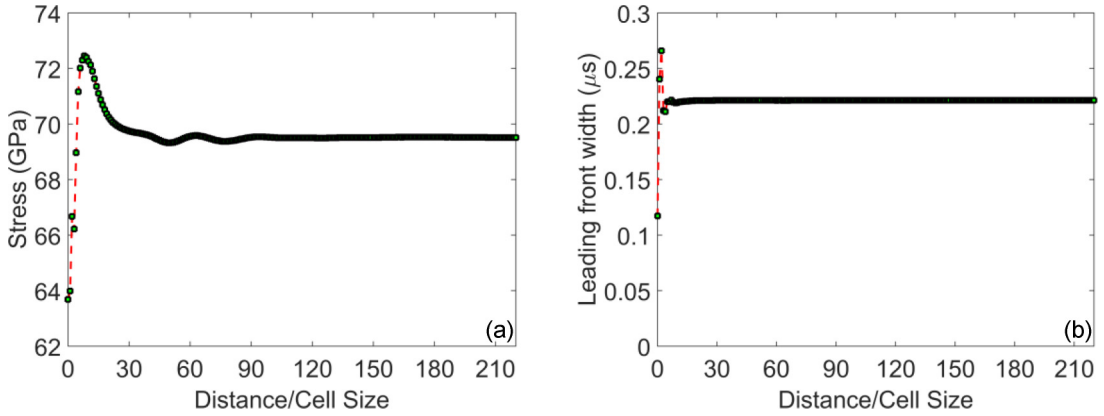

FIG. 16. A 0.5+0.5 laminate impacted by an 80-mm Al flyer plate at 2800 m/s: (a) maximum stress in the leading peak vs propagation distance and (b) leading front width versus propagation distance.

duration of incoming pulse. Figures 18(a) and 18(b) present the profiles of the stress waves in the 0.5+0.5 laminate impacted by an 800-mm Al flyer plate.

It is clear from Fig. 18 that these impact conditions resulted in a steady shock wave. Figure 19 demonstrates that the establishment of the maximum stress and the leading front width of the shock wave happen at the same normalized distances from the impacted end as in the 0.5+0.5 laminate impacted by an 80 mm Al flyer plate. This demonstrates that the establishment of a steady shock front is mainly the result of the laminate mesostructure and the properties of the components and the duration of the relatively long incoming stress pulse has almost no effect.

Comparing Figs. 6(a) and 6(b), Figs. 12(a) and 12(b), and Figs. 18(a) and 18(b), we observe that the period of the elastic oscillations behind the shock front is equal to 0.37 μs for the 0.5+0.5 laminate, 0.75 μs for the 1+1 laminate, and 1.56 μs for the 2+2 laminate. It is clear that the period of these oscillations is directly related to the laminate cell size.

Finally, Fig. 20 shows that the steady shock front width was reached at the same normalized distance (about 30 cells) from the impacted end as the case for the same laminate impacted by the 80-mm Al flyer plate (Fig. 17). It is evident that the cell refinement in the laminate has a direct influence on the establishment of steady shock waves and their characteristic space scales.

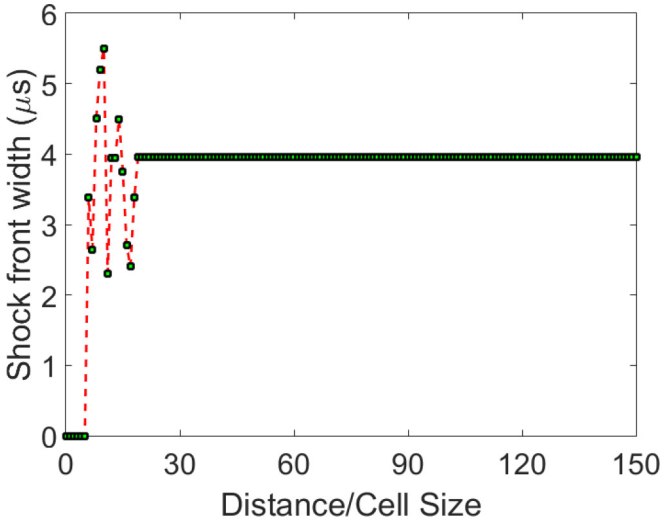

FIG. 17. Shock front width vs traveled distance in a 0.5+0.5 Al laminate impacted by an 80-mm Al flyer plate at 2800 m/s.

The results of the presented numerical simulations demonstrated that quasistationary shock waves are formed when the duration of incoming compression pulse is long enough. These shock waves had a stationary oscillatory profiles connecting the initial and final quasiequilibrium states (it has elastic slow attenuating strain oscillations). We have found that the characteristic cell size of the laminate affects the leading front width and shock front width (both linearly proportional to the cell size of the laminate), while the quasistationary state behind the shock front appears to be independent of the cell size.

It is clear from Figs. 3, 6, 9, and 12 that two mechanisms are responsible for the formation of the stationary leading front: reflection of the leading wave at interfaces, which widens the front (geometrical dispersion), and nonlinearity, which steepens it. The shock front width is influenced by the dissipation (in the case investigated mostly by the viscoplastic behavior of components) and it is an order of magnitude larger than the leading front width determined by the balance of the geometrical dispersion and nonlinear behavior of components.

The observed properties of the qusistationary shock waves are qualitatively similar to the shock waves in the weakly dissipative dispersive system described by the KdV equation [27,28]. In the following section we will attempt to identify a scaling of the main shock parameters using the dissipative KdV approach.

G. Scaling of shock wave parameters using the dissipative KdV equation

Nondissipative elastic periodic laminates support weakly nonlinear small-amplitude solitarylike waves (stegotons) [3]. It was also shown that short-duration high-amplitude stress pulses in the Al-W laminate have properties similar to KdV solitons despite the dissipation due to the plastic deformation. They attenuate while keeping their solitarylike identity determined by the nondissipative KdV equation [4,11].

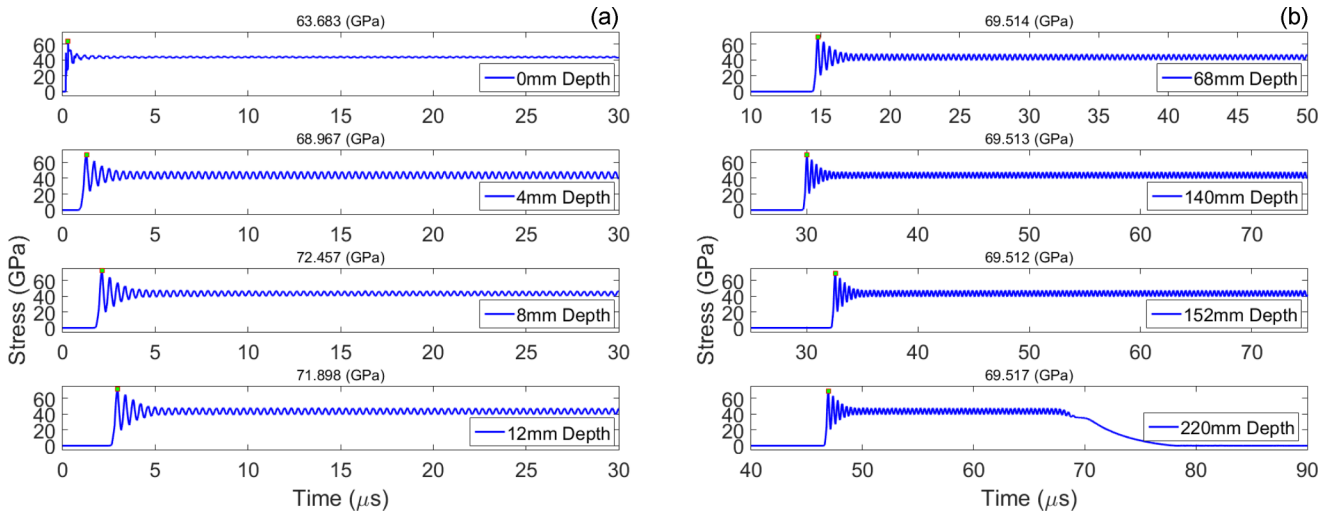

FIG. 18. Evolution of stress wave profiles in a 0.5+0.5 laminate impacted by an 800-mm Al flyer plate at 2800 m/s at different distances from the impacted end: (a) 0, 4, 8, and 12 mm and (b) 68, 140, 152, and 220 mm.

The stationary solution of the nondissipative KdV equation (1) presented below provides a reasonable approximation for the properties of these solitarylike waves:

$$\xi_t + C_0\xi_x + S\xi_{xxx} + \nu\xi\xi_x = 0, \tag{1}$$

$$S = \frac{d^2 C_0}{24}, \tag{2}$$

$$\nu = \frac{\alpha_{\rm eq} C_0}{K_{\rm eq}}, \tag{3}$$

$$C_0^2 = \frac{d^2}{\frac{d_a^2}{C_a^2} + \frac{d_b^2}{C_b^2} + \left(\frac{Z_a}{Z_b} + \frac{Z_b}{Z_a}\right)\left(\frac{d_a d_b}{C_a C_b}\right)}. \tag{4}$$

The cell size d and the long-wave sound speed C_0 in the laminate determine the dispersive coefficient S, and the coefficients $\alpha_{\rm eq}$ and $K_{\rm eq}$ are responsible for the nonlinear behavior of the laminate under compression. The parameters $\alpha_{\rm eq}$ and $K_{\rm eq}$ for the high-amplitude stress pulses were found using the Hugoniot curve of the components ($D_i = C_{0i} + s_i u_i$), allowing an approximation of the stress-strain relation of the laminate at high stresses (the subscript i identifies the Al or W component). This approach results in the following expression for the parameters $\alpha_{\rm eq}$ and $K_{\rm eq}$ (details how to find them can be found in [4]),

$$K_{\rm eq} = \frac{K_{\rm Al} K_{\rm W}}{(1-\tau)K_{\rm Al} + \tau K_{\rm W}}, \tag{5}$$

$$\alpha_{\rm eq} = \frac{\tau K_{\rm W}^3 \alpha_{\rm Al} + (1-\tau)K_{\rm Al}^3 \alpha_{\rm W}}{[(1-\tau)K_{\rm Al} + \tau K_{\rm W}]^3}, \tag{6}$$

where τ is the volume fraction of Al. The coefficients $K_{\rm i}$ and α_i (i stands for Al or W) for each component are

$$K_i = \frac{C_{0i}^2}{V_{0i}}, \tag{7}$$

$$\alpha_i = \frac{2 s_i C_{0i}^2}{V_{0i}}, \tag{8}$$

where V_{0i} represents the specific volume of Al or W. As mentioned before, K and α capture the linear and nonlinear stress-strain behavior under compression; these coefficients have been determined using the material's shock Hugoniot (a detailed explanation can be found in [4]).

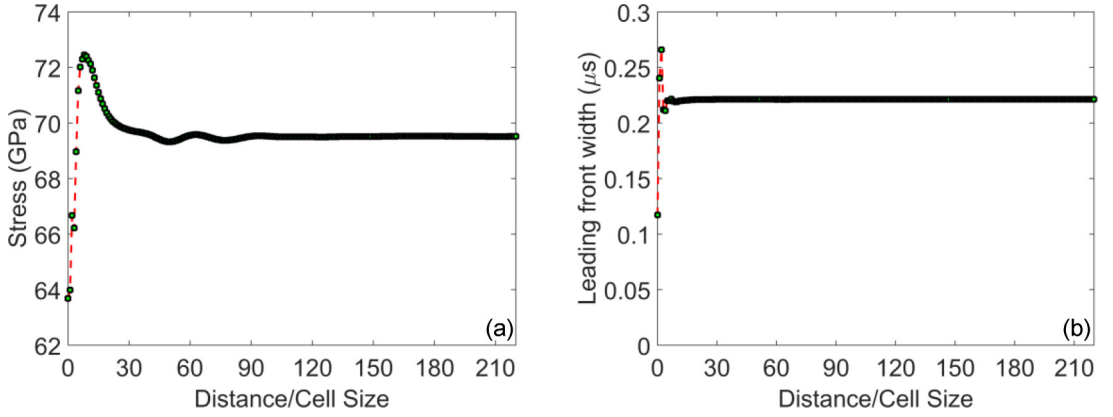

FIG. 19. (a) Maximum stress in the leading peak vs propagation distance and (b) leading front width versus propagation distance in a 0.5+0.5 laminate impacted by an 800-mm Al flyer plate at 2800 m/s.

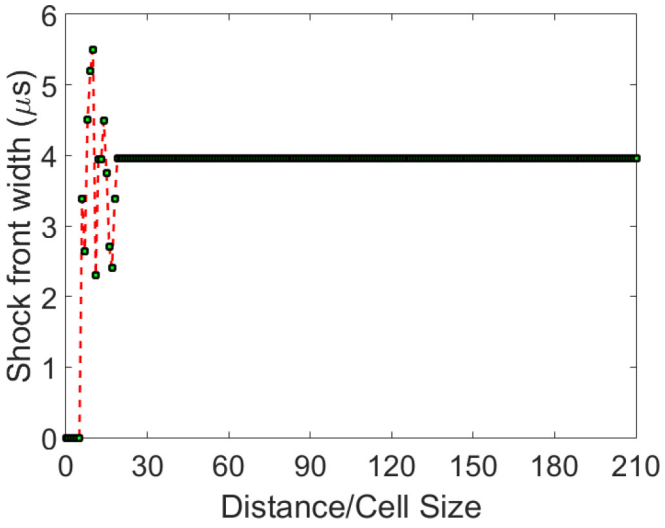

FIG. 20. Shock front width vs traveled distance in a 0.5+0.5 laminate impacted by an 800-mm Al flyer plate at 2800 m/s.

Equation (1) has the following solitary solution propagating with speed v:

$$\xi = \xi_m \mathrm{sech}^2\left[\left(\frac{2\alpha_{\mathrm{eq}}\xi_m}{d^2 K_{\mathrm{eq}}}\right)^{1/2}(x - vt)\right]. \tag{9}$$

Attenuating short-duration high-amplitude stress pulses at given strain amplitude ξ_m can be approximated by this equation [4,11].

The results of the numerical calculations presented above demonstrate that the incoming, long-duration, high-amplitude stress pulses generate stationary oscillatory shock waves (e.g., Figs. 6, 12, and 18). It is natural to explore if the parameters of these shock waves can be described by adding dissipation properties to the KdV equation (1).

The KdV equation with a viscous dissipative term (where μ is the viscosity coefficient) is

$$\xi_t + C_0\xi_x + S\xi_{xxx} + \nu\xi\xi_x - \mu\xi_{xx} = 0. \tag{10}$$

Equation (10) not only predicts the attenuating quasistationary solitarylike waves, but also supports a different type of disturbance: a stationary shocklike wave [27,28].

The shocklike strain wave supported by Eq. (10) has some specific properties that we will compare with the results of numerical calculations presented above. First, the speed of propagation of this shocklike wave depends on its amplitude

$$V_{\mathrm{sh}} = C_0 + \frac{\alpha_{\mathrm{eq}} C_0}{2K_{\mathrm{eq}}}\xi_f, \tag{11}$$

where ξ_f is the strain in the final state behind the shock wave.

It is important to note that the speed of the shocklike stress wave is independent of the nature of dissipation; for example, in the Al-W laminate, it is mostly due to the plastic deformation and not due to the viscosity. Depending on the dissipation level, the shock structure in nonlinear materials with a periodic mesostructure can be oscillatory (weakly dissipative) or monotonic (strongly dissipative) [27,28], but in both cases, the speed of the wave can be found using Eq. (11).

Second, the profile of the shocklike solution for the weakly dissipative equation (10) has three characteristic space scales. The shocklike strain wave profile can be described by the equation in the reference system moving with the speed of the shock wave V_{sh} [27,28],

$$\xi = \xi_f + \mathrm{const}\exp\left(\frac{\mu}{2S}x\right)\cos\left(\sqrt{\frac{\nu\xi_f}{2S}}x\right), \tag{12}$$

where the leading shock front is at $x = 0$, ξ_f is the final strain behind shock, and the shock wave propagates to the right ($x < 0$).

This equation clearly demonstrates the existence of three spatial scales. One is related to the leading front width ($\pi\sqrt{S/2\nu\xi_f}$). This scale is of similar order of magnitude to the scale of the solitarylike wave supported by the nondissipative KdV equation (1). It was demonstrated that this scale is related to the shape of the high-amplitude localized waves in Al-W laminates having properties similar to the KdV solitary waves [4]. The second, larger scale ($2\pi\sqrt{2S/\nu\xi_f}$) is related to the period of decaying oscillations behind the leading front, where the plastic work is still present. The third characteristic scale $2S/\mu$ is related to the spatial rate of decay of the oscillation amplitude, determined by the viscosity and the dispersion coefficient. It is important to note that first two scales depend linearly on the characteristic space scale of the mesostructure d. However, the third characteristic scale, related to the oscillations amplitude decay, is proportional to d^2.

The change from an oscillatory to a monotonic shocklike profile, supported by the weakly nonlinear KdV equation (10), is determined by the critical value of viscosity μ_{cr} [27] given by

$$\mu_{\mathrm{cr}} = \sqrt{2S\nu\xi_f}. \tag{13}$$

The critical value of viscosity can be also identified for a strongly nonlinear periodic system of particles interacting by the Hertz law [1]. It is expected that a monotonic profile will be observed in the case of the strongly dissipative wave propagating in periodic structures with other mechanisms of dissipation, e.g., laminates with layers of foam [2] or metal plates separated by rubber O rings [29].

Another important property of the stationary oscillating shock wave solution of the weakly nonlinear dissipative KdV equation (10) is that the maximum amplitude of strain in the leading pulse is equal to 1.5 of the final strain in the case when dissipation is very weak (and the leading pulse is very close to the solitarylike wave) [27]. It is interesting to compare the presented properties of the shocklike solution of Eq. (10) with the results of numerical calculations demonstrating oscillatory shock profiles (Figs. 6, 12, and 18).

The speed of the steady shock waves with different amplitude, strains in their leading maximum, the final mean strain in the quasiequilibrium state, and their ratio obtained in numerical calculations are presented in Table I. These data correspond to the 2+2 laminate impacted by an Al flyer plate of 800 mm thickness at different velocities. Table I also presents theoretical values of speed for the shocklike stress wave (corresponding to the final mean strains from a

TABLE I. Speed of shock waves with different amplitude, strains in their leading maximum, a final mean strain in quasiequilibrium states, their ratio obtained in numerical calculations, theoretical values of speed for shocklike stress wave, and the difference between theoretical and numerical values of shock wave speeds. The data correspond to a 2+2 laminate impacted by an Al flyer plate of 800 mm thickness at different velocities.

2+2 Al-W laminate						
Impactor velocity (m/s)	Shock speed (m/s)	Maximum strain on leading front	Mean final strain in a quasiequilibrium state	Ratio of maximum to final mean strain	Theoretical speed (m/s)	Difference between theoretical and numerical values of shock speed
2800	4729	0.2762	0.2003	1.4	4605.4	2.7%
2400	4542	0.2354	0.174	1.4	4445	2.2%
2000	4363	0.1962	0.1473	1.3	4281.6	1.9%
1600	4180	0.1541	0.1199	1.3	4114.2	1.6%

numerical calculations) and the difference between theoretical [using Eq. (11)] and numerical values of shock wave speeds.

We can see that the theoretical values for the speed of the shocklike stress waves obtained using Eq. (11) are close to their values in numerical calculations (the maximum difference is 2.7%). The ratio of the strain amplitude in the leading maximum and the mean strain at the final state for different amplitudes of shock waves is in the interval 1.3–1.4, being only slightly lower than the predicted value for weakly dissipative and weakly nonlinear KdV equations. This demonstrates that plastic deformation in Al-W laminates results in a weakly dissipative behavior of stress pulses.

It is interesting to compare the shape of the localized stress pulses (excited by impact of an 8-mm Al flyer plate at 2800 m/s), leading fronts of the shocklike waves (excited by impact of 80 mm Al flyer plate and 800 mm Al flyer plate at 2800 m/s) in numerical calculations, and the solitary wave solution of Eq. (1) with similar amplitude. This comparison is presented in Fig. 21, which clearly shows that the solitary solution of Eq. (1) provides a correct estimation of the spatial characteristics of the localized stress pulse and the leading part of the shocks at their similar stress amplitudes.

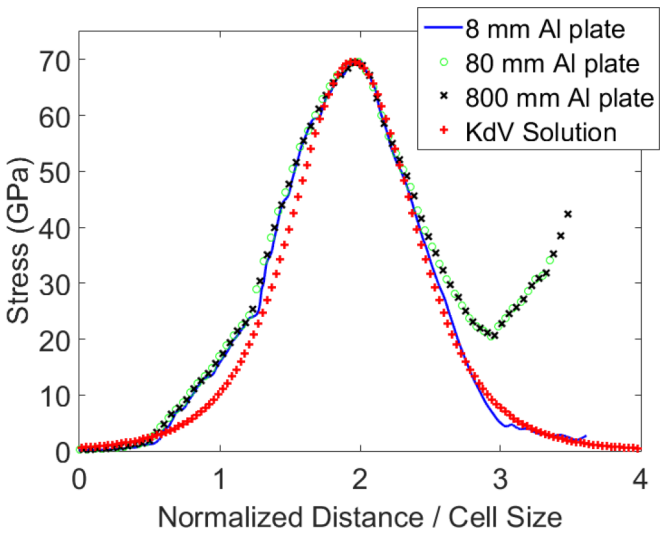

FIG. 21. Comparison of the KdV solitary solution to the shape of the localized stress pulse (excited by impact of an 8-mm Al flyer plate) and the leading part of the shock wave with similar amplitude excited by impact of an 80-mm Al flyer plate and an 800-mm Al flyer plate. All cases correspond to a 2+2 Al-W laminate and an impactor velocity of 2800 m/s.

The period of decaying oscillations on the back of the leading front of the shock wave in the KdV approach is related to the amplitude and dispersive properties of the laminate scaling linearly with the cell size [Eq. (12)]. These periods ($2\pi\sqrt{2S/\nu\xi_f}$) for similar values of ξ_f are equal to 0.0084, 0.0042, and 0.0021 m for 2+2, 1+1, and 0.5+0.5 laminates, respectively, scaling with the sizes of the unit cells.

From numerical simulations we obtain the following values for these periods of decaying oscillations: 0.0079, 0.0039, and 0.0019 m, corresponding to the 2+2, 1+1, and 0.5+0.5 laminates. It is clear that the periods of the oscillations in the numerical calculations (Figs. 6, 12, and 18) are close to the data from the theoretical approach based on the KdV equation. They are close to being proportional to the cell size. This again demonstrates that the high-amplitude oscillatory shock waves in the Al-W laminates are weakly dissipative and scaled with the cell size, as in the theoretical approach, despite the qualitatively different mechanisms of dissipation.

The rate of the amplitude decay of the oscillations in the leading part of the shock wave in the weakly dissipative KdV approach is related to the viscosity and the dispersive coefficient (12) and it has a characteristic space scale $2S/\mu$ that is proportional to the square of the cell size. The results of the amplitude decay of the oscillations for the different laminates are shown in Fig. 22. Figure 22 compares the decay of the first four oscillations in different laminates (2+2, 1+1, and 0.5+0.5) under the same impact by the 800-mm Al flyer plate with a velocity of 2800 m/s. It is clear that the space scale corresponding to their decay from the leading maximum to a point where only the elastic oscillations exist scales almost linearly with the cell size [Fig. 22(a)].

This scaling is different from expected from the dissipative KdV approach with a constant viscosity. It indicates that the mechanism of plastic deformation in laminates cannot be described by an effective viscosity coefficient that does not depend on the spatial scale d. This is expected because attenuation in the laminate is also due to wave reverberations and at given distance the number of these reverberations depends on the cell size d. Based on the numerical results, we can conclude that if the dissipative mechanism is to be described by the effective viscosity this parameter should be proportional to d.

The elastic oscillations in the region behind the shock front width demonstrate a very low rate of decay [Figs. 6, 12, and 18). Their periods are equal to 0.0074, 0.0035, and 0.0017 m for the 2+2, 1+1, and 0.5+0.5 laminates scaled by their cell sizes. It is clear that these very slowly decaying oscillations are

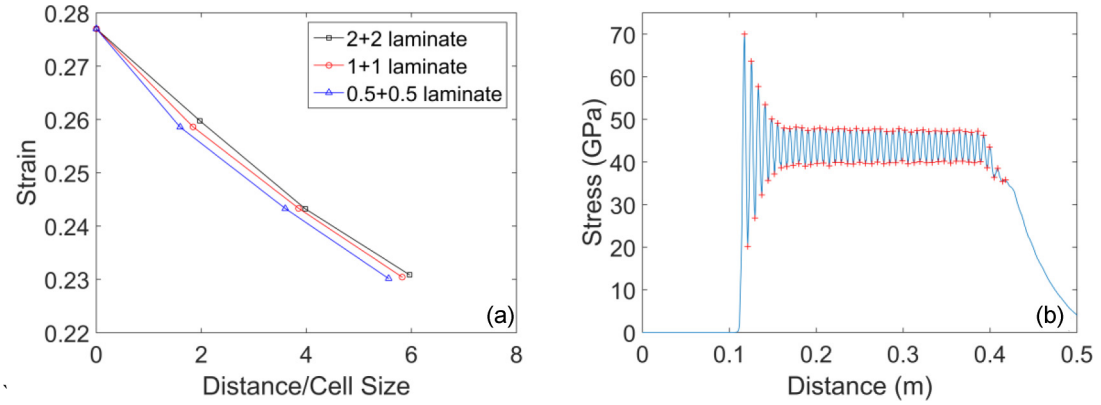

FIG. 22. (a) Decay rate of the first four oscillations on the leading shock on 2+2, 1+1, and 0.5+05 laminates. (b) Oscillating shock on a 2+2 laminate that shows the decay of the oscillations until a quasiequilibrium state has been reached.

not described by the proposed KdV approach with a constant viscosity. It might be described with an effective viscosity vanishing or dramatically reduced at a certain level of stress below the yield stress.

The nonlinearity taken into account in the proposed KdV approach for the Al-W laminates is based only on the nonlinear relation between stresses and strains for each component determined by the interatomic forces. The nonlinear parameters of the components and the subsequent nonlinear parameter of the laminate under compression were found from their shock Hugoniots as most representative for the material behavior under the investigated stress amplitudes. The detailed explanation of the procedure used can be found in [4]. Numerical calculations include all mechanisms of nonlinearity (the nonlinear relation between stresses and strains and convective and geometric nonlinearities), but our simplified KdV approach still is able to provide a reasonable description of the numerical results and scaling of the leading front thickness responsible for the maximum strain rates in shocked laminates.

IV. CONCLUSION

Long-duration impulse loading (compared to the characteristic time scale of the laminate) of the Al-W laminate resulted in the formation of oscillatory steady shock waves in Al-W laminates with different mesostructure. The width of the leading front and the maximum strain rates due to shock loading are determined by the dispersive and nonlinear parameters of the laminate and not by dissipation, as is the case in uniform solids. The characteristic spatial scale of the leading shock front can be satisfactory described by the Korteweg–de Vries approximation as well as its speed and the ratio of the maximum to final strain. The dissipation determines a shock front width where multiple loading-unloading cycles bring the laminate into a final quasiequilibrium state. The period of the fast decaying oscillations is well described by the KdV approach and scales linearly with the cell size of the laminate. The rate of decay of these oscillations in the numerical calculations does not scale with the square of the cell size, as expected from the dissipative KdV approach with a constant viscosity due to the different mechanism of dissipation in high-amplitude compression pulses.

ACKNOWLEDGMENTS

P.F.N. thanks Consejo Nacional de Ciencia y Tecnología (407461) and The University of California Institute for Mexico and the United States for the funding provided to make this work possible.

[1] E. B. Herbold and V. F. Nesterenko, Propagation of Rarefaction Pulses in Discrete Materials with Strain-Softening Behavior, Phys. Rev. Lett. **110**, 144101 (2013).

[2] V. F. Nesterenko, *Dynamics of Heterogeneous Materials* (Springer Science & Business Media, New York, 2001).

[3] D. H. Yong and R. J. LeVeque, Solitary waves in layered nonlinear media, SIAM J Appl. Math. **63**, 1539 (2003).

[4] P. Franco Navarro, D. J. Benson, and V. F. Nesterenko, Nature of short, high-amplitude compressive stress pulses in a periodic dissipative laminate, Phys. Rev. E **92**, 062917 (2015).

[5] R. Kinslow, *High-Velocity Impact Phenomena* (Elsevier, New York, 2012).

[6] S. P. Marsh, *LASL Shock Hugoniot Data* (University of California Press, Berkeley, 1980), Vol. 5.

[7] R. McQueen, S. Marsh, and J. Fritz, Hugoniot equation of state of twelve rocks, J. Geophys. Res. **72**, 4999 (1967).

[8] C. Wei, B. Maddox, A. Stover, T. Weihs, V. Nesterenko, and M. Meyers, Reaction in Ni-Al laminates by laser-shock compression and spalling, Acta Mater. **59**, 5276 (2011).

[9] C. Wei, V. Nesterenko, T. Weihs, B. Remington, H.-S. Park, and M. Meyers, Response of Ni/Al laminates to laser-driven compression, Acta Mater. **60**, 3929 (2012)

[10] O. E. Petel and F. X. Jetté, Comparison of methods for calculating the shock hugoniot of mixtures, Shock Waves **20**, 73 (2010).
[11] P. Franco Navarro, D. J. Benson, and V. F. Nesterenko, Proceedings of the 19th Biennial Conference on Shock Compression of Condensed Matter (in press).
[12] V. Nesterenko, V. Fomin, and P. Cheskidov, Damping of strong shocks in laminar materials, J. Appl. Mech. Tech. Phys. **24**, 567 (1983).
[13] D. Benson and V. Nesterenko, Anomalous decay of shock impulses in laminated composites, J. Appl. Phys. **89**, 3622 (2001).
[14] R. Hofmann, D. J. Andrews, and D. Maxwell, Computed shock response of porous aluminum, J. Appl. Phys. **39**, 4555 (1968).
[15] J. W. Swegle and D. E. Grady. Shock viscosity and the prediction of shock wave rise times, J. Appl. Phys. **58**, 692 (1985).
[16] A. Molinari and G. Ravichandran, Fundamental structure of steady plastic shock waves in metals, J. Appl. Phys. **95**, 1718 (2004).
[17] A. Molinari and G. Ravichandran, Modeling plastic shocks in periodic laminates with gradient plasticity theories, J. Mech. Phys. Solids **54**, 2495 (2006).
[18] D. E. Grady, Structured shock waves and the fourth-power law, J. Appl. Phys. **107**, 013506 (2010).
[19] D. E. Grady, Unifying role of dissipative action in the dynamic failure of solids, J. Appl. Phys. **117**, 165905 (2015).
[20] S. Zhuang, G. Ravichandran, and D. E. Grady, An experimental investigation of shock wave propagation in periodically layered composites, J. Mech. Phys. Solids **51**, 245 (2003).
[21] J. O. Hallquist, *LS-DYNA Theory Manual* (Livermore Software Technology Corporation, Livermore, 2006); http://www.lstc.com/pdf/ls-dyna_theory_manual_2006.pdf
[22] D. Steinberg, S. Cochran, and M. Guinan, A constitutive model for metals applicable at high-strain rate, J. Appl. Phys. **51**, 1498 (1980).
[23] D. Steinberg, *Equation of State and Strength Properties of Selected Materials* (Lawrence Livermore National Laboratory, Livermore, 1996).
[24] L. C. Chhabildas and J. R. Asay, Rise-time measurements of shock transitions in aluminum, copper and steel, J. Appl. Phys. **50**, 2749 (1979).
[25] J. C. Crowhurst, M. R. Armstrong, K. B. Knight, J. M. Zaug, and E. M. Behymer, Invariance of the Dissipative Action at Ultrahigh Strain Rates Above the Strong Shock Threshold, Phys. Rev. Lett. **107**, 144302 (2011).
[26] S. Y. Wang and V. F. Nesterenko, Attenuation of short strongly nonlinear stress pulses in dissipative granular chains, Phys. Rev. E **91**, 062211 (2015).
[27] V. Karpman, *Nonlinear Waves in Dispersive Media* (Pergamon, New York, 1975).
[28] R. Z. Sagdeev, Fine structure of a shock-wave front propagated across a magnetic field in a rarefied plasma, Sov. Phys. Tech. Phys. **6**, 867 (1962).
[29] X. Yichao and V. F. Nesterenko, Proceedings of the 19th Biennial Conference on Shock Compression of Condensed Matter (Ref. [11]).